

ISSN 0065-3713

INSTITUT D'AERONOMIE SPATIALE DE BELGIQUE

3 - Avenue Circulaire  
B - 1180 BRUXELLES

## AERONOMICA ACTA

A - N° 325 - 1988

Temperature dependence of ultraviolet absorption  
cross-sections of chlorofluoro-ethanes

by

P.C. Simon, D. Gillotay, N. Vanlaethem-Meuree and J. Wisemberg

BELGISCH INSTITUUT VOOR RUIMTE-AERONOMIE

3 - Ringlaan  
B - 1180 BRUSSEL

## **FOREWORD**

The paper entitled "Temperature dependence of ultraviolet absorption cross-sections of chlorofluoroethanes" is submitted for publication in "Annales Geophysicae".

## **AVANT-PROPOS**

L'article intitulé "Temperature dependence of ultraviolet absorption cross-sections of chlorofluoroethanes" est soumis pour publication dans la revue "Annales Geophysicae".

## **VOORWOORD**

Het artikel "Temperature dependence of ultraviolet absorption cross-sections of chlorofluoroethanes" is voorgelegd ter publikatie in "Annales Geophysicae".

## **VORWORT**

Der Artikel "Temperature dependence of ultraviolet absorption cross-sections of chlorofluoroethanes" ist zur Veröffentlichung vorgelegt in "Annales Geophysicae".

TEMPERATURE DEPENDENCE OF ULTRAVIOLET ABSORPTION  
CROSS-SECTIONS OF CHLOROFUORO-ETHANES

P.C. SIMON, D. GILLOTAY, N. VANLAETHEM-MEUREE and J. WISEMBERG

ABSTRACT

New absorption cross-sections of three haloethanes ( $C_2F_5Cl$ ,  $C_2F_4Cl_2$  ( $CF_2Cl-CF_2Cl$ ), and  $C_2F_3Cl_3$  ( $CF_2Cl-CFCl_2$ )) measured between 172 and 250 nm for temperatures ranging from 225 to 295 K, are presented with uncertainties between 2 and 4 %. They are compared with previous measurements available at room temperature and at only one low temperature, namely 208 K.

The largest temperature effects which take place near the absorption threshold, can amount up to 50 % for  $C_2F_3Cl_3$  and 70% for  $C_2F_4Cl_2$ ; temperature effect, if any, was too small to be detected in the case of  $C_2F_5Cl$ . Extrapolated values for temperatures of aeronomical interest are presented as well as parametrical formulae which give absorption cross-section values for given wavelength and temperature useful in stratospheric modelling calculations.

Photodissociation coefficients are presented and their temperature dependence is discussed.

## RESUME

Des nouvelles valeurs de sections efficaces d'absorption de trois haloéthanes ( $C_2F_5Cl$ ,  $C_2F_4Cl_2$  ( $CF_2Cl-CF_2Cl$ ) et  $C_2F_3Cl_3$  ( $CF_2Cl-CFCl_2$ ) mesurées entre 172 et 250 nm pour des températures comprises entre 225 et 295 K, sont présentées avec une incertitude comprise entre 2 et 4%. Elles sont comparées avec des déterminations antérieures réalisées à température ambiante et à une basse température, 208 K.

L'effet de température le plus important, qui a lieu près du seuil d'absorption, peut atteindre 50% pour  $C_2F_3Cl_3$  et 70% pour  $C_2F_4Cl_2$ ; l'effet de température, s'il existe, est trop faible pour être mis en évidence dans le cas de  $C_2F_5Cl$ .

Les valeurs extrapolées aux températures d'intérêt aéronomique sont présentées de même que des équations paramétriques permettant de calculer des valeurs de sections efficaces d'absorption pour des intervalles de longueur d'onde et de température donnés. Les coefficients de photodissociation sont donnés et leur dépendance en température est discutée.

## SAMENVATTING

Nieuwe werkzame absorptiedoorsneden van drie haloëthanen ( $C_2F_5Cl$ ,  $C_2F_4Cl_2$  ( $CF_2Cl$  -  $CF_2Cl$ ), en  $C_2F_3Cl_3$  ( $CF_2Cl$  -  $CFCl_2$ ) gemeten tussen 172 en 250 nm voor temperaturen schommelend tussen 225 en 295 K, worden voorgesteld met onzekerheden tussen 2 en 4%. Ze worden vergeleken met vorige metingen die bij kamertemperatuur bereikt worden en slechts bij één lage temperatuur, namelijk 208 K.

De belangrijkste temperatuurgevolgen die optreden bij de absorptiedrempel kunnen 50% bereiken voor  $C_2F_3Cl_3$  en 70% voor  $C_2F_4Cl_2$ ; temperatuurgevolg, als dit bestaat, was te onbeduidend om opgespoord te worden bij  $C_2F_5Cl$ .

Geëxtrapoleerde waarden voor temperaturen van aëronomisch belang worden voorgesteld, alsook parametrische formules die toelaten waarden te berekenen van werkzame absorptiedoorsneden voor gegeven golflengten en temperaturen. De fotodissociatiecoëfficiënten worden gegeven en hun temperatuurafhankelijkheid wordt besproken.

## ZUSAMMENFASSUNG

Neue Absorptionsdurchquerschnitten von drei Haloethanen ( $C_2F_5Cl$ ,  $C_2F_4Cl_2$  ( $CF_2Cl$  -  $CF_2Cl$ ), und  $C_2F_3Cl_3$  ( $CF_2Cl$  -  $CFCl_2$ )) gemessen zwischen 172 und 250 nm für Temperaturen wechselnd zwischen 225 und 295 K, werden vorgestellt mit Unsicherheiten zwischen 2 und 4%. Vergleichungen werden gemacht mit vorhergehenden Messungen erreicht bei Zimmertemperatur und nur bei einer geringen Temperatur, nämlich 208 K.

Die wichtigste Temperaturfolgen die auftreten bei der Absorptionschwelle können 50% erreichen für  $C_2F_3Cl_3$  und 70% für  $C_2F_4Cl_2$ ; Temperaturfolge, wenn sie besteht, war zu unbedeutend um ermittelt zu werden bei  $C_2F_5Cl$ .

Extrapolierte Werten für Temperaturen von aeronomischem Interesse werden vorgestellt, wie auch parametrische Vergleichungen die zulassen Werten zu berechnen von Absorptionsdurchquerschnitten für gegeben Wellenlänge und Temperaturen. Die Fotodissoziationskoeffizienten werden gegeben und die Temperaturabhängigkeit wird besprochen.

## INTRODUCTION

Amongst the numerous halocarbons of industrial origin released to the atmosphere and considered as potentially harmful for stratospheric ozone, halomethanes like  $\text{CCl}_4$ ,  $\text{CHCl}_3$ ,  $\text{CH}_2\text{Cl}_2$ ,  $\text{CH}_3\text{Cl}$ ,  $\text{CFCl}_3$ ,  $\text{CF}_2\text{Cl}_2$ ,  $\text{CF}_3\text{Cl}$ ,  $\text{CHFCl}_2$ ,  $\text{CHF}_2\text{Cl}$ , ... and haloethanes like  $\text{CH}_3\text{CCl}_3$  (Vanlaethem et al., 1979) or  $\text{C}_2\text{F}_5\text{Cl}$  (CFC-115),  $\text{C}_2\text{F}_4\text{Cl}_2$  ( $\text{CF}_2\text{ClCF}_2\text{Cl}$ , CFC-114) and  $\text{C}_2\text{F}_3\text{Cl}_3$  (CFC $\text{Cl}_2\text{CF}_2\text{Cl}$ , CFC-113) are currently recognized as the halocarbons likely to have the most significant impacts on stratospheric ozone in the foreseeable future.

The most important chlorofluoroethanes seem to be CFC-113, CFC-114 and CFC-115. Indeed, Singh et al. (1979) concluded that the residence time of these later halocarbons is at least several decades, and that photolysis in the stratosphere would be the major sink. This was confirmed by the calculations of Wuebbles (1983), and by recent measurements of concentration profiles (Borchers et al. 1987, Fabian et al. 1981, Penkett et al. 1981).

The reliability of such predictions is strongly dependent on the photodissociation pattern adopted for these haloethanes. Until now, three sets of measurements of absorption cross-sections are available at room temperature (Robbins 1976; Chou et al. 1978 and Hubrich and Stuhl 1980). For the two first determinations, the proposed values disagree for CFC-115 by about 50% over the 186 - 204 nm wavelength range. Moreover, the measurements of Hubrich and Stuhl (1980), in the case of CFC-114, disagree by at least 30% with the values proposed by Robbins (1976) and Chou et al. (1978).

The absorption cross-sections were also measured for the three compounds at only one low temperature, namely 208 K, by Hubrich and Stuhl (1980).

The purpose of this paper is to report a new investigation of the ultraviolet absorption spectrum of CFC-113, CFC-114 and CFC-115 over

the wavelength range 172-230 nm, and for temperature between 295 and 225 K. Temperature dependence of the absorption cross-sections of CFC-113 and CFC-114 is clearly shown. Photodissociation coefficients are calculated and their temperature dependence is discussed.

Parametrical equations are also given to derive absorption cross-section values for wavelength and temperature ranges used in stratospheric modelling calculations.

### EXPERIMENTAL

The three chlorofluoroethanes were obtained after distillation under vacuum from commercially available analytical grade products manufactured by Kali Chemie and evaporated from the gas-handling system in pyrex to the absorption cell.

The absorption measurements have been performed by mean of a thermostatic stainless absorption cell with a 2 m optical path. It can be evacuated down to  $10^{-7}$  torr by an ion pump which prevents any contamination. Low temperature regulation down to 220 K was obtained by pumping cooled methylcyclohexane through double jacket around the absorption cell. Thermal equilibrium was usually obtained after 3 or 4 hours with a maximum temperature gradient between both ends of the cell of 2 K at 220 K. The pressure was monitored by capacitance manometers MKS Baratron directly connected to the absorption cell. Three different heads covered pressures ranging from  $10^{-4}$  to 1000 torr with a precision better than 0.1 %. The pressure decrease was followed during each refrigeration process. The actual gas temperature was determined by considering both the conditions prevailing at the three points of measurement in the cell and the value deduced from the pressure decrease, according to the perfect gas law.

An EMR 542 P.09.18 solar blind photomultiplier was used a detector of the incident and transmitted fluxes, a deuterium source and a 1 m model 225 Mc Pherson monochromator providing the monochromatic incident radiation.

A more complete description of the experimental device has been given previously by Wisemberg and Vanlaethem (1978) and by Gillotay and Simon (1988).

Determination of the absorption cross-sections is made after at least ten consistent sequential recordings of the incident and absorbed fluxes measured for identical temperature conditions, using the Beer-Lambert's law :

$$I(\lambda) = I_0(\lambda) \exp(-\sigma(\lambda) n d) \quad (1)$$

where :  $I_0(\lambda)$  and  $I(\lambda)$  are respectively the incident and transmitted fluxes,

$n$  is the number of molecules per volume unit,

$d$  is the optical path, and

$\sigma(\lambda)$  is the absorption cross-section

In all cases, the validity of Beer-Lambert's law was confirmed over the pressure ranges used for absorption measurements and specified in table 4.

At ambient temperature, the quoted accuracy is of the order of  $\pm 2\%$ , but at lower temperatures, the RMS uncertainties increased from  $\pm 3\%$  to  $\pm 4\%$  for the absorption cross-sections values lower than  $2 \times 10^{-21} \text{ cm}^2 \text{ molec}^{-1}$ .

## RESULTS

The absorption spectra are shown in Fig. 1 and 2. Numerical values of the corresponding absorption cross-sections for selected wavelengths between 174 and 250 nm (namely 2 nm intervals) and wave-number intervals of  $500 \text{ cm}^{-1}$ , currently used for aeronomy modelling (Brasseur and Simon, 1981) are respectively given in tables 1a-3a and 1b-3b.

### a) Ambient temperature (295 K).

Chlorofluoroethanes display continuous absorption in the 172-230 nm region, with absorption cross-sections ranging from  $10^{-18}$  to

$10^{-22} \text{ cm}^2 \text{ molec.}^{-1}$ . The progressive substitution of F atoms of the basic hexafluoroethane by Cl atoms leads to increased absorption and extends the absorption region towards longer wavelengths.

Cross-section measurements have been extended to longer wavelengths than those currently available (namely to  $3.6 \times 10^{-22} \text{ cm}^2 \text{ molec.}^{-1}$  for CFC 113 and  $2 \times 10^{-22} \text{ cm}^2 \text{ molec.}^{-1}$  for CFC 115).

The new results are presented in Fig. 1. with the available cross-section values published by Robbins (1976) and Chou et al. (1978) and Hubrich (1980) for comparison purposes . The discrepancies between the previous cross-section values are clearly illustrated, showing, in the case of  $\text{C}_2\text{F}_5\text{Cl}$ , differences up to 50% between the measurements of Robbins (1976) and Chou et al. (1978) over the wavelength range 186-204 nm, the values of Hubrich and Stuhl (1980) being 10% higher than those of Robbins. The cross-section values reported here confirm those reported by Robbins (1976). For  $\text{C}_2\text{F}_3\text{Cl}_3$  we confirm the values reported by Chou et al. (1978) and Hubrich and Stuhl (1980). In the case of  $\text{C}_2\text{F}_4\text{Cl}_2$ , the new measurements resolve the remaining inconsistencies between Chou et al. (1978) and Robbins (1976) at, for instance, 195 and 212 nm. The values proposed by Hubrich and Stuhl (1980) are in average 30% higher than all other available data. Interpolated values of new absorption cross-section measurements at 2 nm intervals are listed in tables 1-3.

b) Low temperature (225 K - 270 K).

It can be seen from Fig. 2., that absorption cross-sections decrease with temperature by a factor which depends on both the wavelength and the chemical composition of the compound. This effect is most significant at low temperatures, in the vicinity of low absorptions, and in the case of  $\text{C}_2\text{F}_4\text{Cl}_2$ . It progressively disappears in the region of high absorptions. Temperature effects, if any, were too small to be detected in our experimental conditions in the case of  $\text{C}_2\text{F}_5\text{Cl}$ .

For all compounds, the analysis of the relationship of absorption cross-sections versus temperature for a given wavelength shows an exponential decrease in the considered wavelength and temperature ranges. (Fig. 3.) Because the temperature range 225-295 K is

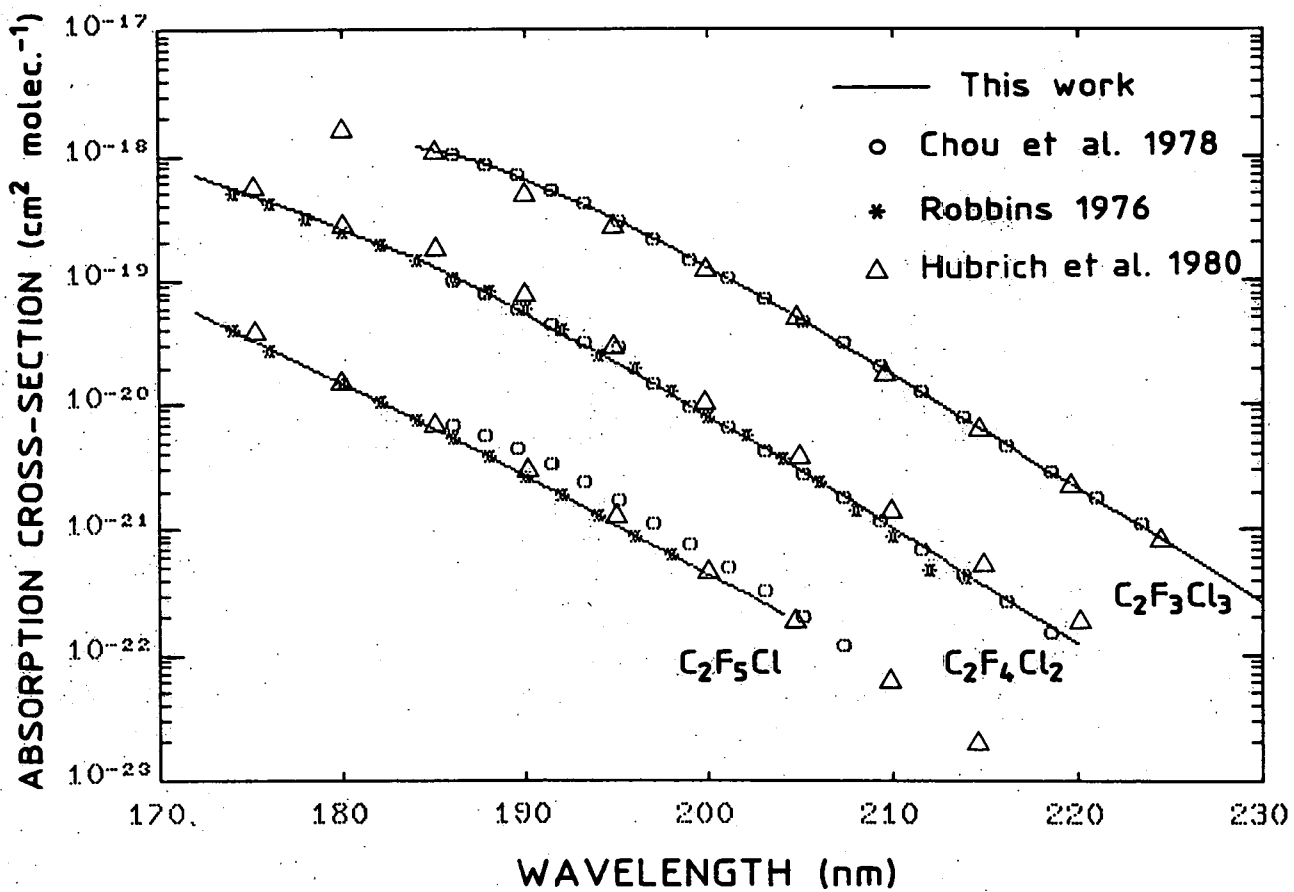


Fig. 1.- Ultraviolet absorption cross-sections of  $\text{C}_2\text{F}_3\text{Cl}_3$ ,  $\text{C}_2\text{F}_4\text{Cl}_2$  and  $\text{C}_2\text{F}_5\text{Cl}$  with respect of wavelength at 295 K.

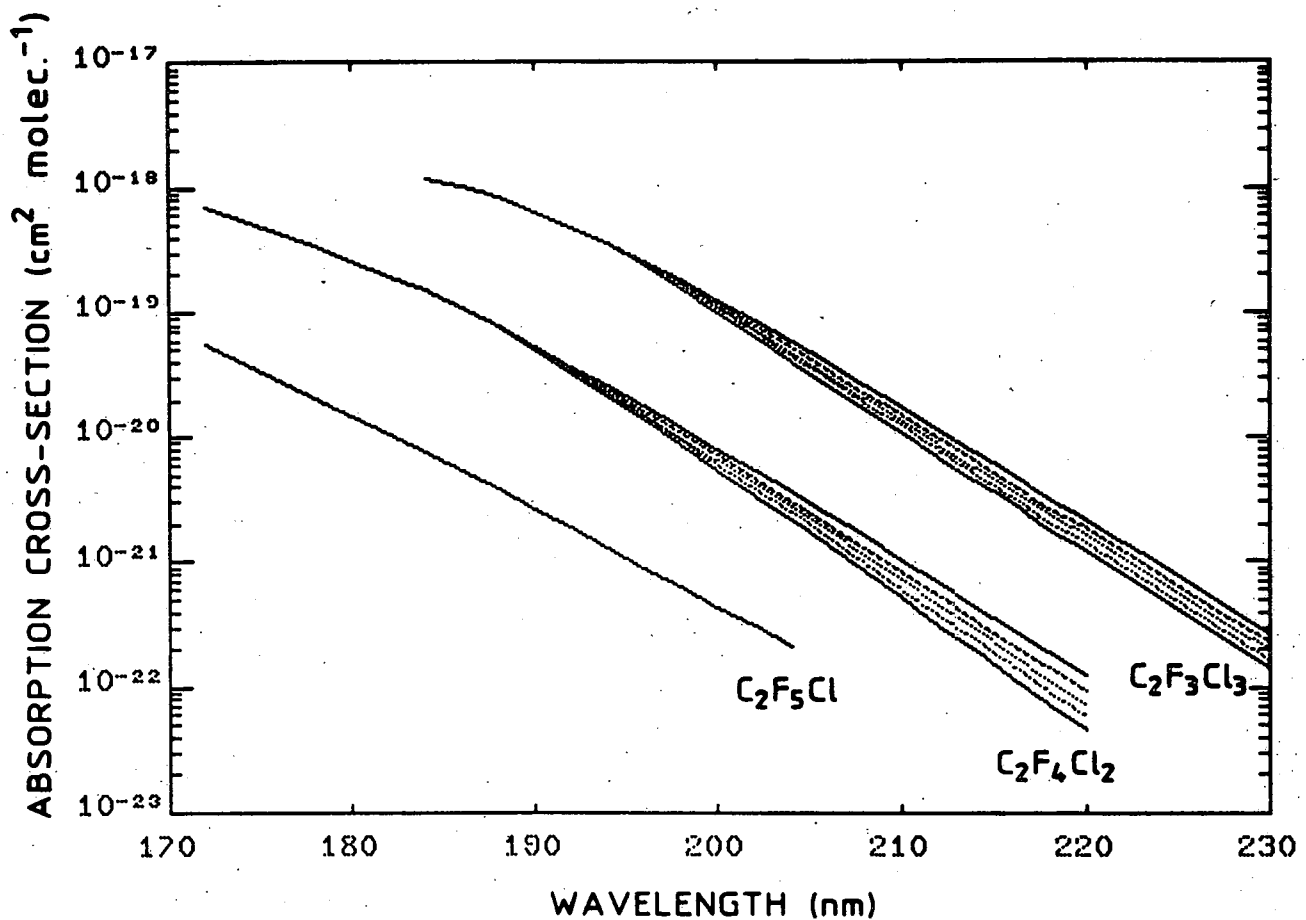


Fig. 2.- Ultraviolet absorption cross-sections of  $\text{C}_2\text{F}_3\text{Cl}_3$ ,  $\text{C}_2\text{F}_4\text{Cl}_2$  and  $\text{C}_2\text{F}_5\text{Cl}$  versus wavelength as a function of temperature (T = 295 K, 270 K, 250 K, 230 K and 210 K).

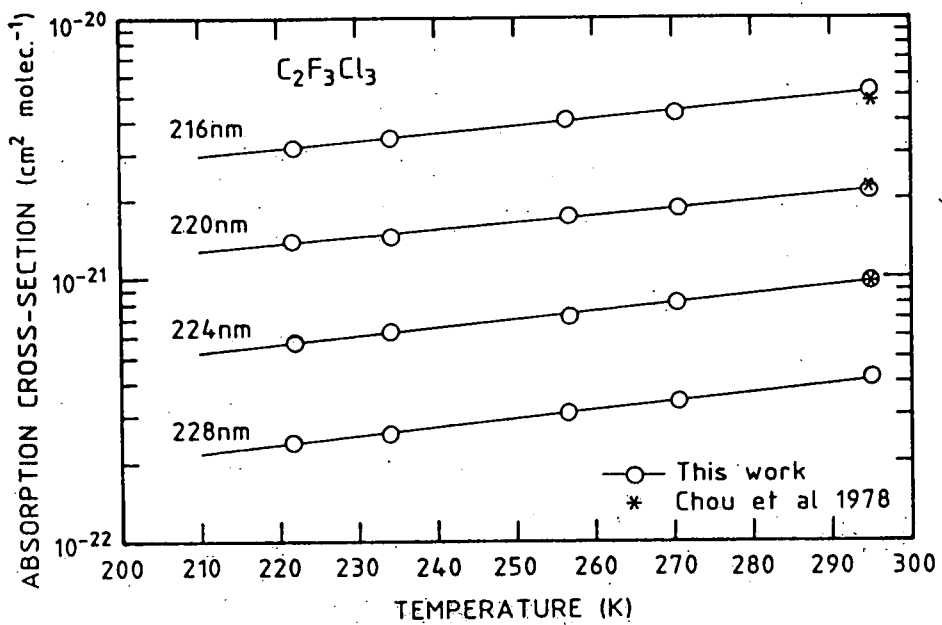
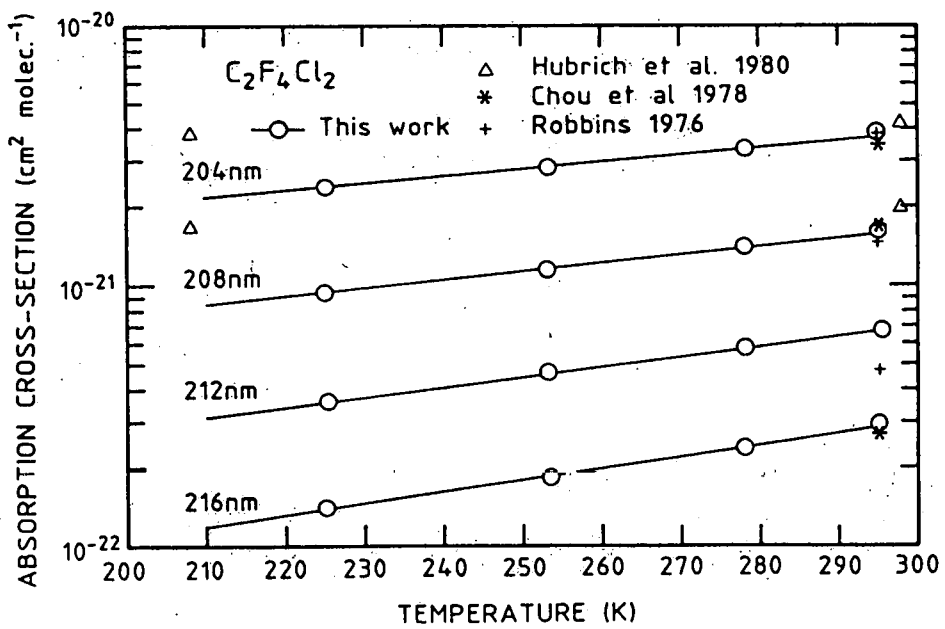


Fig. 3.- Absorption cross-sections of  $\text{C}_2\text{F}_3\text{Cl}_3$  and  $\text{C}_2\text{F}_4\text{Cl}_2$  versus temperature at four wavelengths.

adequately covered by accurate measurements performed at four different temperatures around 225, 255, 270 and 295 K, extrapolation down to 210 K can be accurately made as well as interpolation at selected temperatures.

Numerical values deduced from a least square fit through the four temperatures measured are presented in tables 1-3 for four defined temperatures (270, 250, 230, 210 K) which cover the usual stratospheric temperature conditions.

A similar study has already been made at only one low temperature (208 K) in a 10 cm optical path cell, by Hubrich and Stuhl (1980). They qualitatively find similar temperature effects than those presented here. They are in fairly good agreement for  $C_2F_3Cl_3$  expected at 195 nm, as can be seen on figure 4. In the case of  $C_2F_4Cl_2$ , the effect measured by Hubrich and Stuhl (1980) is lower than these reported here. Moreover, they find a slight temperature effect  $C_2F_5Cl$  which is not observed in our experimental conditions. Discrepancies can be explained by a critical analysis of the experimental conditions reported by Hubrich and Stuhl (1980) which reveals quoted accuracy up to  $\pm 50\%$  in the wavelength range where temperature effects are the most important.

In addition, in our experimental conditions, absorption cross-section measurements for which transmitted fluxes are higher than 90% or lower than 10% have been rejected in order to maintain the quoted accuracy over the whole wavelength range.

Because of the exponential dependence of the absorption cross-sections ( $\sigma$ ) with temperature (T) at each wavelength ( $\lambda$ ), the following empirical function between those parameters can be defined :

$$\log_{10} \sigma(\lambda) = A(\lambda) + B(\lambda) \times T \quad (2)$$

where the coefficients  $A(\lambda)$  and  $B(\lambda)$  were determined by a polynomial fitting of the available experimental data with respect of temperature and wavelength by mean of a least squares algorithm developed by The Math

Works Inc. (PC - MATLAB), according to the following polynomial expression :

$$\log_{10} \sigma(\lambda, T) = A_0 + A_1 \lambda + \dots + A_n \lambda^n + (T-273) \times (B_0 + B_1 \lambda + \dots + B_n \lambda^n) \quad (3)$$

The computed values of the  $A_i$  and  $B_i$  coefficients are given in table 5.

The calculated values of absorption cross-sections deduced from expression (3) are in agreement with all the experimental data within 4%.

### DISCUSSION

As discussed by Sandorfy (1976), the continuous absorption of chlorofluoroethanes in the 200 nm region corresponds to the less energetic band of their electronic spectrum. It is due to the existence of a  $(C-Cl)^* \leftarrow \overline{Cl}$  transition involving excitation to a repulsive electronic state (C-Cl antibonding). Substitution of hydrogen on the basic hydrocarbon entity by Cl atoms leads to an increased absorption and a red shift of the average wavelength absorption range, while F atoms play the opposite role and stabilize the molecule. Unfortunately, the complexity of the spectrum features, especially in the case of poly-chloro-compounds, makes a theoretical analysis of temperature dependence of their absorption cross-sections very difficult.

Relative values  $\sigma(T)/\sigma(295)$  versus wavelength relationships, for a given temperature, are shown on Fig.4.

It is currently accepted, that the first photodissociation step for all halocarbons in the wavelength and pressures ranges of stratospheric interest is the release of one Cl atom with an unit quantum yield, according to the general scheme :



The rapid reaction of  $RCi_{x-1}$  with atmospheric  $O_2$  releases another Cl atom leaving  $RCi_{x-2}$  which in turn can be subject to photolysis. The ultimate fate of such radicals in stratospheric conditions ought to be considered

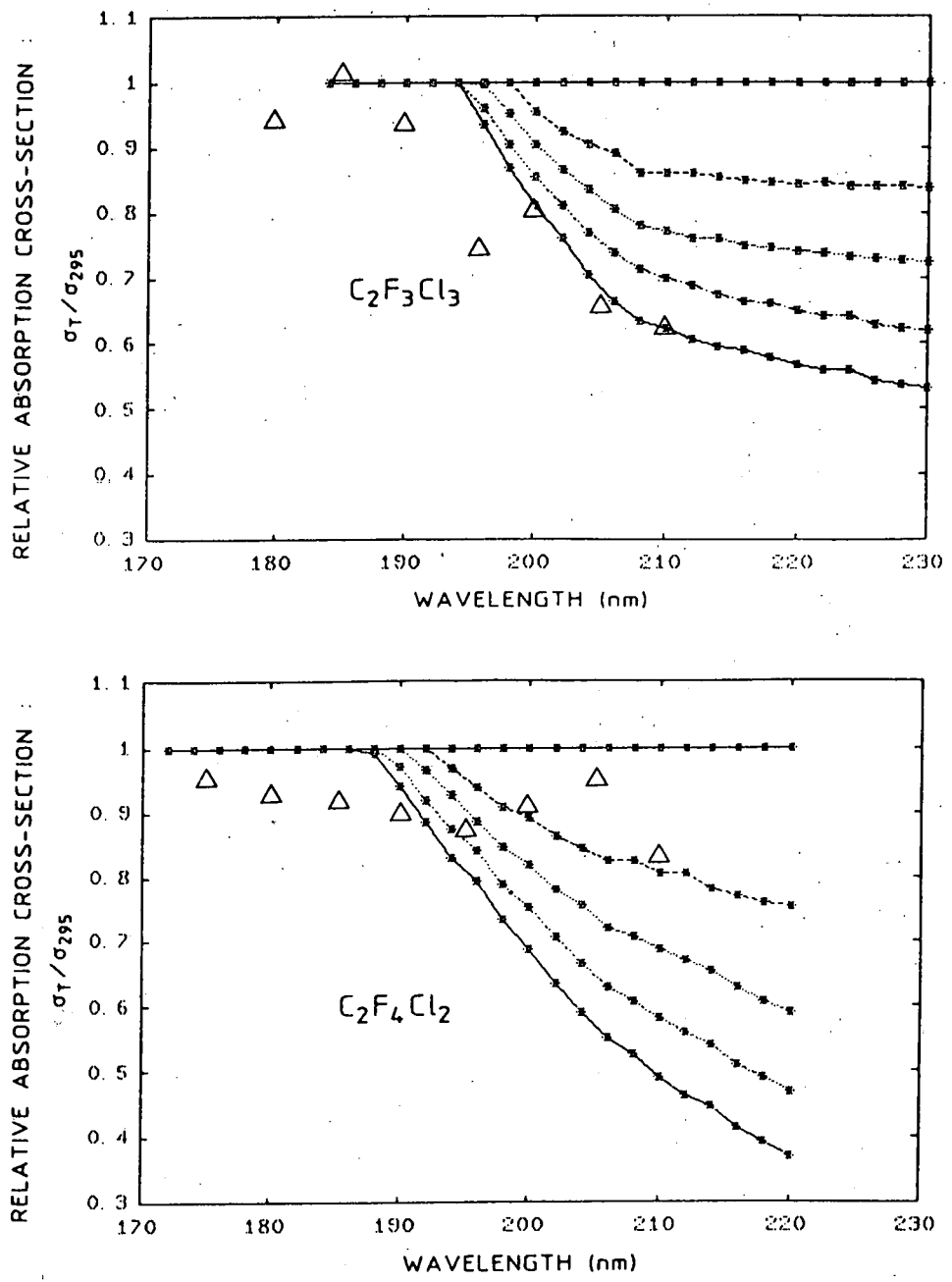


**Fig. 4.** - Relative absorption cross-sections  $\sigma(T)/\sigma(295 \text{ K})$  as a function of wavelength for the twochlorofluoro-ethanes showing a temperature dependence.  
 $(T = 295 \text{ K}, 270 \text{ K}, 250 \text{ K}, 230 \text{ K} \text{ and } 210 \text{ K})$   
 $(\Delta) : \text{Hubrich and Stuhl (1980)} \text{ } T = 208 \text{ K}$

in detail in order to define the average production of ClO radicals due to the photodissociation of each halocarbon.

Photodissociation coefficients  $J$ , neglecting effects of multiple scattering, have been computed for a given altitude ( $z$ ), zenith angle ( $\chi$ ) and wavelength interval according to the relations:

$$J(z) = \sigma_\lambda q_\lambda(z) \quad (5)$$

$$q_\lambda(z) = q_\lambda(\infty) e^{-\tau_\lambda(z)} \quad (6)$$

$$\tau_\lambda(z) = \int_z^\infty [n(O_2) \sigma_\lambda(O_2) + n(O_3) \sigma_\lambda(O_3) + n(\text{air}) \sigma_{\text{scatt.}}] \sec \chi dz \quad (7)$$

where  $\sigma$  are the absorption cross-sections

$q_\lambda(z)$  and  $q_\lambda(\infty)$  are the solar irradiances at altitude  $z$  or extraterrestrial ( $z=\infty$ )

$n$  is the number of particles per volume unit.

for solar zenith angles  $\chi$  of  $0^\circ$  and  $60^\circ$  ( $\sec \chi = 1$  and 2), taking the values of  $\sigma_\lambda(O_2)$ ,  $\sigma_\lambda(O_3)$  from WMO (1985) and Kockarts (1976),  $\sigma_{\text{scatt}}$  from Nicolet (1984) and the values of  $q_\lambda(\infty)$  from WMO (1985) and taking into account the actual values of cross-sections which correspond to the temperature conditions prevailing at a defined altitude (Table 7, Fig. 5 and 6). A comparison of either temperature dependent or independent photodissociation coefficients for different stratospheric altitudes (15 to 50 km) is presented in Fig. 7. where relative photodissociation coefficients  $J(T)/J(295)$  versus altitude relationships are given for studied compounds.

Obviously, the effect is maximum at low altitudes and gradually decreases, following the temperature gradient in the stratosphere. Due to the significant increase of ozone optical depth in the stratosphere at wavelength beyond 220 nm, the value of the overall photodissociation coefficients between 20 and 35 km is mainly influenced by the 200-210 nm

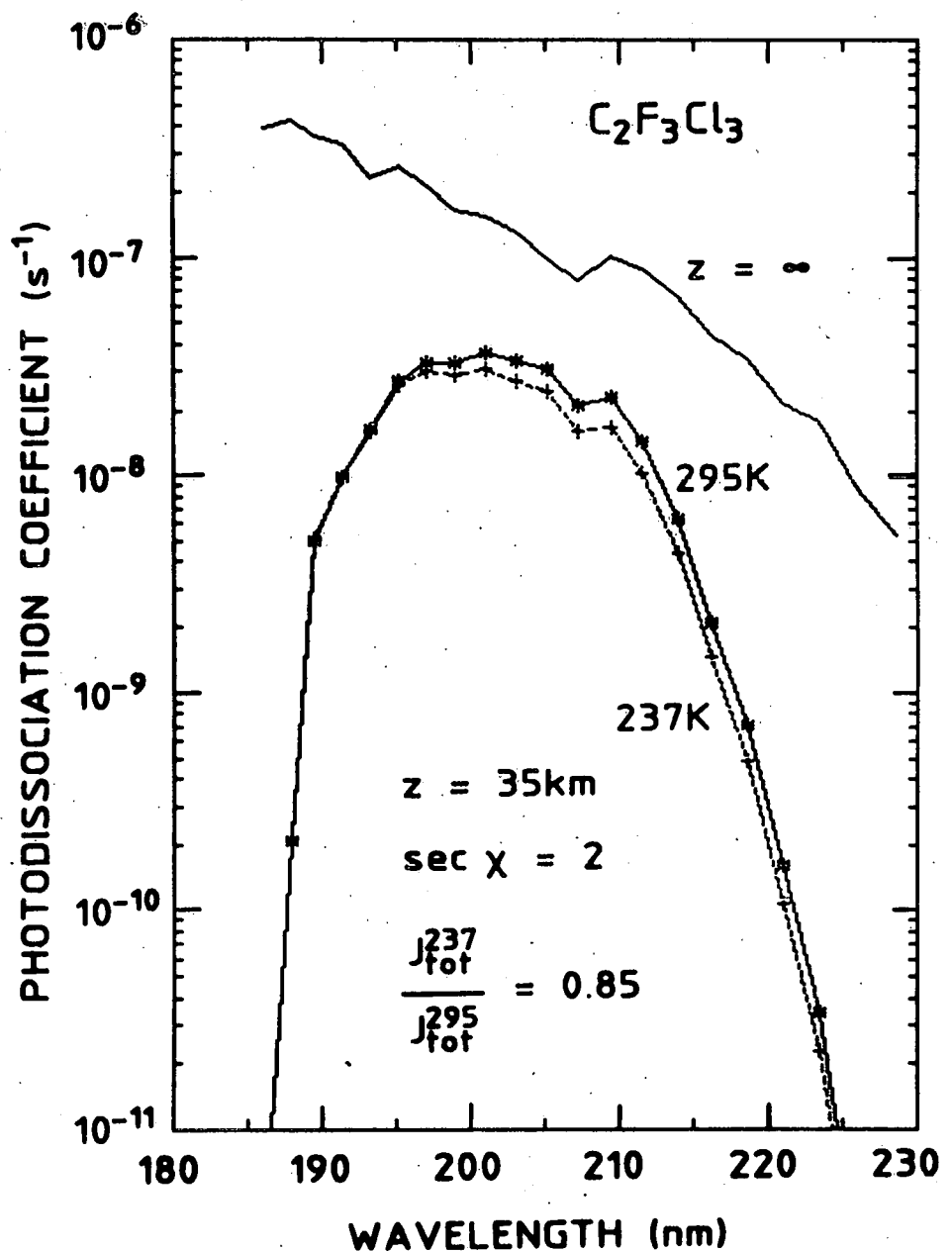


Fig. 5.—Spectral distribution of photodissociation coefficients of  $\text{C}_2\text{F}_3\text{Cl}_3$  for frequency intervals of  $500 \text{ cm}^{-1}$ , for  $z = 35 \text{ km}$  and solar zenith angle =  $60^\circ$  ( $\sec = 2$ ).

(\*) :  $J(295 \text{ K})$ , (+) :  $J(T)$ .

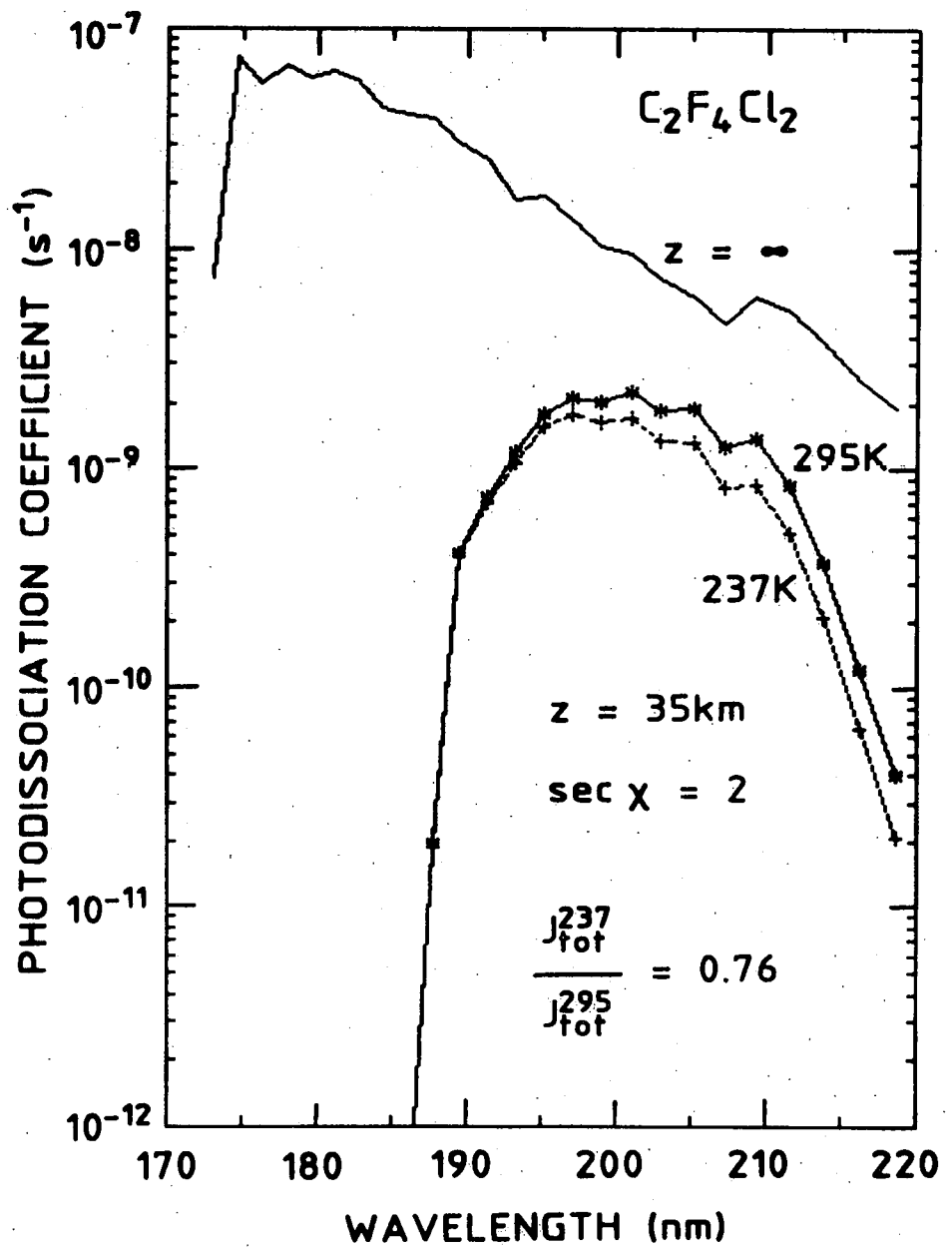


Fig. 6.- Spectral distribution of photodissociation coefficients of  $\text{C}_2\text{F}_4\text{Cl}_2$  for frequency intervals of  $500 \text{ cm}^{-1}$ , for  $z = 35 \text{ km}$  and solar zenith angle =  $60^\circ$  ( $\sec \chi = 2$ ).

(\*) :  $J(295 \text{ K})$  (+) :  $J(T)$ .

interval contribution. In such conditions, a significant reduction of overall photodissociation coefficients is only to be expected in the case of compounds whose absorption cross-sections are strongly temperature dependent in this wavelength interval. Accordingly, important reduction factor are observed for  $C_2F_4Cl_2$  up to 40 % and for  $C_2F_3Cl_3$  up to 30 %, as shown on fig. 7.

The introduction of lower photodissociation coefficients in atmospheric models should significantly increase atmospheric residence times in mean altitudes of photolysis. Therefore, the stratospheric chlorine budget will be affected by new photodissociation rate coefficients taking into account the temperature dependence of chlorofluoroethane absorption cross-sections.

In conclusion, this work presents a complete set of experimental data on the temperature dependence of absorption cross-sections of chlorofluoroethanes. Fairly simple relationships to compute the absorption cross-sections values with respect to temperature and wavelength are proposed. The photodissociation coefficients are calculated and the importance of the temperature dependence of absorption cross-section on their values is clearly demonstrated.

#### ACKNOWLEDGMENTS.

The authors wish to thank Dr. G. Brasseur for helpful discussions and Mr. E. Falise who performed the computer calculations of the photodissociation coefficients. This research has been partially supported by the Commission of European Communities under contract 303-78-1.

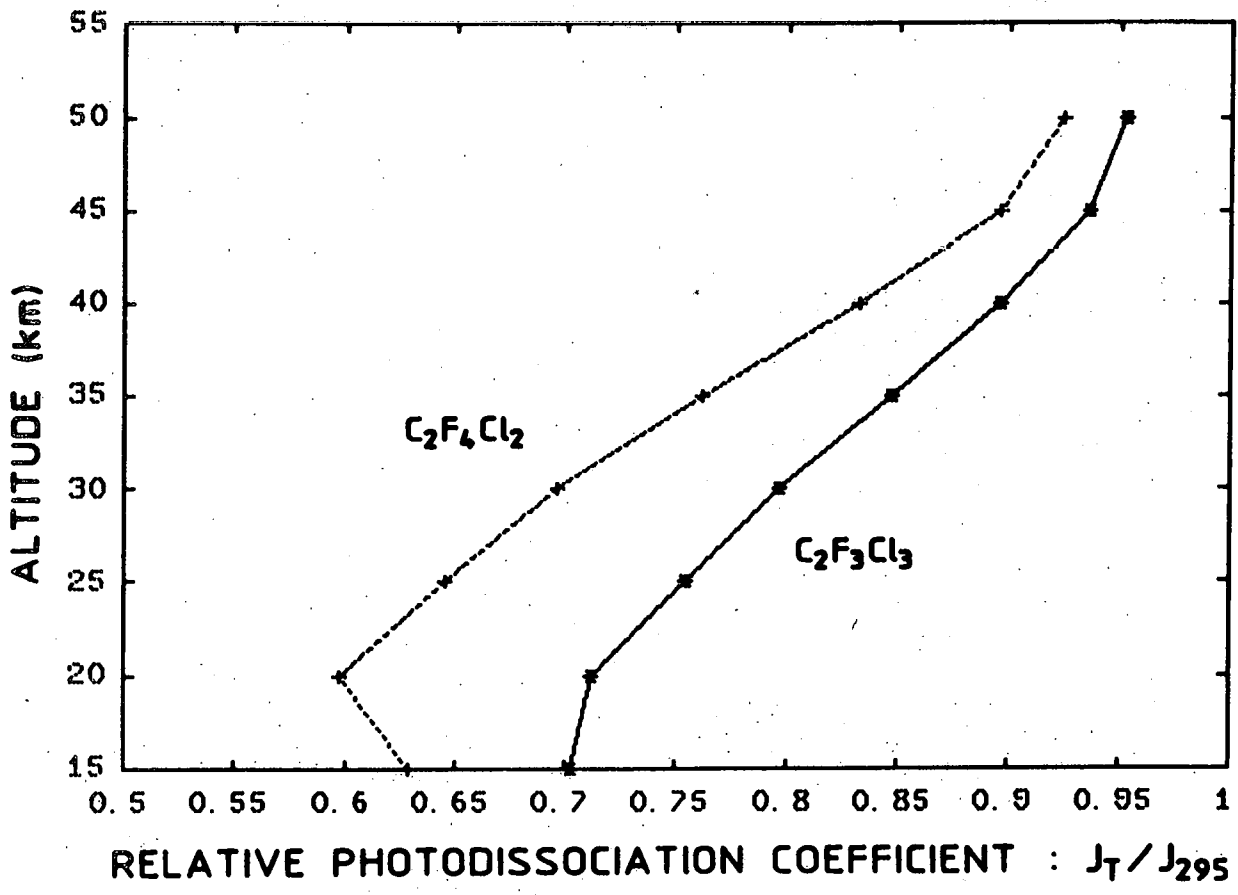


Fig. 7.- Relative photodissociation coefficients  $J(T)/J(295)$  of  $C_2F_3Cl_3$  and  $C_2F_4Cl_2$  as a function of altitude.

REFERENCES.

- BORCHERS, R., P. FABIAN, B.C. KRUGER, S. LAL, U. SCHMIDT, D. KNAPSKA, and S.A. PENKETT, CFC-113( $\text{CCl}_2\text{F}-\text{CClF}_2$ ) in the stratosphere., *Planet. Space Sci.*, 35, 657-663, 1987.
- BRASSEUR, G. and P.C. SIMON, 198Stratospheric and thermal response to long-term variability in solar UV irradiance., *J. Geophys. Res.*, 86, 7343-7362, 1981.
- CHOU, C.C., R.J. MILSTEIN, W.S. SMITH, H. VERA RUIZ, M.J. MOLINA, and F.S. ROWLAND, Stratospheric photodissociation of several saturated perhalo chlorofluorocarbon compounds in current technological use (Fluorocarbons-13, 113, 114, 115)., *J. Phys. Chem.*, 82, 1-7, 1978.
- FABIAN, P., R. BORCHERS, S.A. PENKETT, and N.J.D. PROSSER, Halocarbons in the stratosphere. *Nature*, 294, 733-735, 1981.
- GILLOTAY, D. and P.C. SIMON, Ultraviolet absorption cross-sections of methyl bromide at stratospheric temperatures, *Ann. Geophysicae*, 6, xx-xx, 1988.
- HUBRICH, C. and F. STUHL, The ultraviolet absorption of some halogenated methanes and ethanes of atmospheric interest, *J. Photochem.*, 12, 93-107, 1980.
- KOCKARTS, G. Absorption and Photodissociation in the Schumann-Runge bands of molecular oxygen in the terrestrial atmosphere, *Planet. Space Sci.*, 24, 589-604, 1976.
- NICOLET, M., On the molecular scattering in the terrestrial atmosphere : an empirical formula for calculation in the homosphere, *Planet. Space Sci.*, 32, 1467-1468, 1984.
- PENKETT, S.A., N.J.D. PROSSER, R.A. RASMUSSEN, and M.A.K. KHALIL, Atmospheric measurements of  $\text{CF}_4$  and other fluorocarbons containing the  $\text{CF}_3$  grouping., *J. Geophys. Res.*, 86, 5172-5178, 1981.
- RASMUSSEN, R.A., M.A.K. KHALIL, A.J. CRAWFORD, and P.J. FRASER, Natural and anthropogenic trace gases in the southern hemisphere., *Geophys. Res. Lett.*, 9, 704-707, 1982.

- ROBBINS, D.E., UV photoabsorption cross sections for halocarbons, Int. Conf. on the Stratosphere and related problems, Logan, (USA), 1976 (poster paper).
- SANDORFY, C., Review paper: U.V. absorption of halocarbons, Atm. Environ., 10, 343-351, 1976.
- SINGH, H.B., L.J. SALAS, H. SHIGEISHI, and E. SCRIBNER, Atmospheric halocarbon, hydrocarbons, and sulfur hexafluoride: Global distribution, sources and sinks, Science, E 203F, 899-903, 1979.
- VANLAETHEM-MEUREE, N., J. WISEMBERG and P.C. SIMON, Ultraviolet absorption spectrum of methylchloroform in the vapor phase., Geophys. Res. Lett., 6, 451-454, 1979.
- WISEMBERG, J., and N. VANLAETHEM-MEUREE, Mesures des sections efficaces d'absorption de constituants atmosphériques dans l'ultraviolet: description du système expérimental, Bull. Acad. Roy. Belgique, Cl. Sci., 64, 21-30, 1978.
- WMO, Atmospheric ozone 1985, WMO global ozone research and monitoring project, report 16, Vol. I, 355-367, 1985.
- WUEBBLES, D.J., Chlorocarbon emission scenarios : potential impact on stratospheric ozone, J. Geophys. Res., 88, 1433-1443, 1983.

TABLE 1.a. Absorption cross-sections ( $\sigma(\lambda) \times 10^{21} (\text{cm}^2 \text{ molec.}^{-1})$ ) of  $\text{C}_2\text{F}_3\text{Cl}_3$  at 2 nm interval at selected temperatures (295K, 270 K, 250 K, 230 K, 210 K)

$\lambda$ (nm)	295K	270K	250K	230K	210K
184	1180	1180	1180	1180	1180
186	1040	1040	1040	1040	1040
188	835	835	835	835	835
190	645	645	645	645	645
192	488	488	488	488	488
194	360	360	360	360	360
196	260	260	259	250	243
198	183	183	174	166	159
200	125	119	113	107	101
202	86.0	79.6	74.4	69.7	65.4
204	58.0	52.5	48.4	44.7	40.9
206	40.0	35.6	32.2	29.6	26.6
208	26.5	22.8	20.7	18.9	16.8
210	18.0	15.5	13.9	12.6	11.2
212	11.5	9.89	8.74	7.93	6.96
214	7.60	6.50	5.78	5.13	4.52
216	5.05	4.29	3.79	3.36	2.98
218	3.18	2.69	2.38	2.10	1.84
220	2.20	1.86	1.63	1.43	1.25
222	1.45	1.23	1.07	0.930	0.810
224	0.950	0.800	0.697	0.610	0.530
226	0.630	0.529	0.461	0.396	0.341
228	0.410	0.344	0.299	0.255	0.220
230	0.270	0.226	0.196	0.168	0.144

TABLE 1.b. Absorption cross-sections ( $\sigma(\lambda) \times 10^{21} (\text{cm}^2 \text{ molec.}^{-1})$ ) of  $\text{C}_2\text{F}_3\text{Cl}_3$  over the spectral intervals used in atmospheric modelling calculations (wavenumber interval :  $500 \text{ cm}^{-1}$ ), at selected temperatures (295 K, 270 K, 250 K, 230 K, 210 K)

N°	$\lambda (\text{nm})$	295K	270K	250K	230K	210K
52	185.2-186.9	1040	1040	1040	1040	1040
53	186.9-188.7	860	860	860	860	860
54	188.7-190.5	700	700	700	700	700
55	190.5-192.3	547	547	547	547	547
56	192.3-194.2	415	415	415	415	415
57	194.2-196.1	310	310	310	307	299
58	196.1-198.0	225	225	218	209	202
59	198.0-200.0	158	154	146	138	132
60	200.0-202.0	108	101.5	95.0	89.6	84.2
61	202.0-204.1	73.0	67.0	62.0	57.3	53.3
62	204.1-206.2	48.0	43.0	39.1	36.0	31.7
63	206.2-208.3	31.8	27.8	25.1	23.0	20.7
64	208.3-210.5	19.8	17.1	15.3	14.0	12.4
65	210.5-212.8	12.5	10.7	9.56	8.62	7.56
66	212.8-215.0	7.70	6.58	5.85	5.31	4.58
67	215.0-217.4	4.80	4.08	3.60	3.19	2.83
68	217.4-219.8	2.95	2.49	2.20	1.92	1.70
69	219.8-222.2	1.80	1.50	1.31	1.15	1.00
70	222.2-224.7	1.08	0.900	0.788	0.690	0.600
71	224.7-227.3	0.630	0.529	0.461	0.396	0.341
72	227.3-229.9	0.360	0.302	0.262	0.229	0.192

TABLE 2.a. Absorption cross-sections ( $\sigma(\lambda) \times 10^{21} (\text{cm}^2 \text{ molec.}^{-1})$ ) of  $\text{C}_2\text{F}_4\text{Cl}_2$  at 2 nm interval at selected temperatures (295 K, 270 K, 250 K, 230 K, 210 K)

$\lambda$ (nm)	295K	270K	250K	230K	210K
172	690	690	690	690	690
174	550	550	550	550	550
176	430	430	430	430	430
178	340	340	340	340	340
180	262	262	262	262	262
182	198	198	198	198	198
184	150	150	150	150	150
186	110	110	110	110	110
188	78.0	78.0	78.0	78.0	77.2
190	53.5	53.5	53.5	51.9	50.3
192	37.0	37.0	35.7	34.0	32.8
194	25.6	24.8	23.7	22.4	21.3
196	17.5	16.4	15.5	14.7	13.9
198	12.0	10.9	10.2	9.45	8.80
200	8.00	7.12	6.55	6.03	5.50
202	5.40	4.67	4.21	3.81	3.43
204	3.70	3.12	2.80	2.46	2.18
206	2.45	2.02	1.76	1.54	1.35
208	1.60	1.32	1.13	0.970	0.840
210	1.04	0.837	0.715	0.605	0.510
212	0.680	0.548	0.455	0.380	0.315
214	0.440	0.343	0.287	0.237	0.196
216	0.290	0.223	0.182	0.148	0.120
218	0.190	0.144	0.115	0.0930	0.0740
220	0.122	0.0920	0.0720	0.0570	0.0450

TABLE 2.b. Absorption cross-sections ( $\sigma(\lambda) \times 10^{21} \text{ cm}^2 \text{ molec.}^{-1}$ ) of  $\text{C}_2\text{F}_4\text{Cl}_2$  over the spectral intervals used in atmospheric modelling calculations (wavenumber interval :  $500 \text{ cm}^{-1}$ ), at selected temperatures (295 K, 270 K, 250 K, 230 K, 210 K)

Nº	$\lambda$ (nm)	295K	270K	250K	230K	210K
44	172.4-173.9	610	610	610	610	610
45	173.9-175.4	518	518	518	518	518
46	175.4-177.0	421	421	421	421	421
47	177.0-178.6	347	347	347	347	347
48	178.6-180.2	281	281	281	281	281
49	180.2-181.8	228	228	228	228	228
50	181.8-183.5	182	182	182	182	182
51	183.5-185.2	143	143	143	143	143
52	185.2-186.9	110	110	110	110	110
53	186.9-188.7	80.0	80.0	80.0	80.0	80.0
54	188.7-190.5	58.2	58.2	58.2	57.0	55.3
55	190.5-192.3	42.1	42.1	41.3	39.4	37.9
56	192.3-194.2	30.0	29.4	28.2	26.9	25.7
57	194.2-196.1	20.5	19.6	18.6	17.5	16.5
58	196.1-198.0	14.5	13.4	12.6	11.7	10.9
59	198.0-200.0	9.80	8.82	8.13	7.50	6.91
60	200.0-202.2	6.60	5.77	5.28	4.78	4.03
61	202.0-204.1	4.08	3.49	3.12	2.77	2.49
62	204.1-206.2	2.95	2.46	2.30	1.90	1.68
63	206.2-208.3	1.90	1.56	1.35	1.16	1.01
64	208.3-210.5	1.19	0.963	0.821	0.690	0.595
65	210.5-212.8	0.740	0.588	0.492	0.411	0.348
66	212.8-215.0	0.450	0.351	0.290	0.238	0.198
67	215.0-217.4	0.278	0.214	0.174	0.142	0.114
68	217.4-219.8	0.165	0.124	0.0990	0.0790	0.0630

TABLE 3.a. Absorption cross-sections ( $\sigma(\lambda) \times 10^{21}$  ( $\text{cm}^2 \text{ molec.}^{-1}$ )) of  
 $\text{C}_2\text{F}_5\text{Cl}$  at 2 nm interval.

(nm)	295 K
172	56.5
174	40.5
176	28.5
178	20.5
180	14.5
182	10.5
184	7.50
186	5.35
188	3.85
190	2.70
192	1.90
194	1.30
196	0.900
198	0.630
200	0.440
202	0.310
204	0.210

TABLE 3.b. Absorption cross-sections ( $\sigma(\lambda) \times 10^{21} \text{ cm}^2 \text{ molec.}^{-1}$ ) of  $\text{C}_2\text{F}_5\text{Cl}$  over the spectral intervals used in stratospheric modelling calculations (wavenumber interval :  $500 \text{ cm}^{-1}$ ).

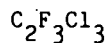
N°	$\lambda$ (nm)	295K
44	172.4-173.9	47.0
45	173.9-175.4	36.2
46	175.4-177.0	27.5
47	177.0-178.6	20.5
48	178.6-180.2	16.0
49	180.2-181.8	12.5
50	181.8-183.5	9.40
51	183.5-185.2	8.20
52	185.2-186.9	5.35
53	186.9-188.7	4.00
54	188.7-190.5	4.95
55	190.5-192.3	2.15
56	192.3-194.2	1.50
57	194.2-196.1	1.06
58	196.1-198.0	0.750
59	198.0-200.0	0.520
60	200.0-202.0	0.360
61	202.0-204.1	0.250

TABLE 4. Experimental conditions for the measurement of absorption cross-sections at low temperatures.

	Temperature range (K).	Max. working pressure (torrs)	Wavelength range showing temperature dependence (nm)
$C_2F_3Cl_3$	: 295-225	: 2.8	: 196-230
	:	:	:
$C_2F_4Cl$	: 295-225	: 35	: 188-220
	:	:	:
$C_2F_5Cl$	: 295-225	: 308	: / - /

\* : at the lowest working temperature.

TABLE 5. Parameters  $A_i$  and  $B_i$  for polynomial function (see formula (3) in the text).

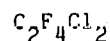


$$\begin{array}{lll} A_0 = -1087.9 & : & B_0 = 12.493 \\ A_1 = 20.004 & : & B_1 = -2.3937 \cdot 10^{-1} \\ A_2 = -1.3920 \cdot 10^{-1} & : & B_2 = 1.7142 \cdot 10^{-3} \\ A_3 = 4.2828 \cdot 10^{-4} & : & B_3 = -5.4393 \cdot 10^{-6} \\ A_4 = -4.9384 \cdot 10^{-7} & : & B_4 = 6.4548 \cdot 10^{-9} \end{array}$$

T range : 210 - 300 K

$\lambda$  range : 182 - 230 nm

---



$$\begin{array}{lll} A_0 = -160.50 & : & B_0 = -1.5296 \\ A_1 = 2.4807 & : & B_1 = 3.5248 \cdot 10^{-2} \\ A_2 = -1.5202 \cdot 10^{-2} & : & B_2 = -2.9951 \cdot 10^{-4} \\ A_3 = 3.8412 \cdot 10^{-5} & : & B_3 = 1.1129 \cdot 10^{-6} \\ A_4 = -3.4373 \cdot 10^{-8} & : & B_4 = -1.5259 \cdot 10^{-9} \end{array}$$

T range : 210 - 300 K

$\lambda$  range : 172 - 220 nm

---



$$\begin{array}{lll} A_0 = 5.8281 & : & B_0 = 0 \\ A_1 = -2.9900 \cdot 10^{-1} & : & B_1 = 0 \\ A_2 = 1.3525 \cdot 10^{-3} & : & B_2 = 0 \\ A_3 = -2.6851 \cdot 10^{-6} & : & B_3 = 0 \end{array}$$

T range : 210 - 300 K

$\lambda$  range : 172 - 204 nm

---

TABLE 6. Temperature model

Altitude (km)	Temperature (K)
15	217
20	217
25	222
30	227
35	237
40	251
45	265
50	271

TABLE 7. Photodissociation coefficients versus altitude

$C_2F_3Cl_3$

Z(km)	sec $\chi = 1$			sec $\chi = 2$		
	$J(s^{-1})$	$J(s^{-1})$	$J_{rel}$	$J(s^{-1})$	$J(s^{-1})$	$J_{rel}$
	$\sigma(295K)^a$	$\sigma = f(T)$		$\sigma(295K)^a$	$\sigma = f(T)$	
15	$8.793 \cdot 10^{-10}$	$6.447 \cdot 10^{-10}$	.732	$2.216 \cdot 10^{-12}$	$1.557 \cdot 10^{-12}$	.702
20	$1.137 \cdot 10^{-8}$	$8.271 \cdot 10^{-9}$	.727	$2.084 \cdot 10^{-10}$	$1.484 \cdot 10^{-10}$	.712
25	$7.335 \cdot 10^{-8}$	$5.707 \cdot 10^{-8}$	.778	$5.201 \cdot 10^{-9}$	$3.921 \cdot 10^{-9}$	.754
30	$2.897 \cdot 10^{-7}$	$2.385 \cdot 10^{-7}$	.823	$5.552 \cdot 10^{-8}$	$4.420 \cdot 10^{-8}$	.796
35	$7.730 \cdot 10^{-7}$	$6.730 \cdot 10^{-7}$	.871	$2.932 \cdot 10^{-7}$	$2.483 \cdot 10^{-7}$	.847
40	$1.482 \cdot 10^{-6}$	$1.352 \cdot 10^{-6}$	.913	$8.686 \cdot 10^{-7}$	$7.783 \cdot 10^{-7}$	.896
45	$2.120 \cdot 10^{-6}$	$2.006 \cdot 10^{-6}$	.946	$1.557 \cdot 10^{-6}$	$1.458 \cdot 10^{-7}$	.936
50	$2.565 \cdot 10^{-6}$	$2.461 \cdot 10^{-6}$	.959	$2.127 \cdot 10^{-6}$	$2.028 \cdot 10^{-6}$	.953

$C_2F_4Cl_2$

Z(km)	sec $\chi = 1$			sec $\chi = 2$		
	$J(s^{-1})$	$J(s^{-1})$	$J_{rel}$	$J(s^{-1})$	$J(s^{-1})$	$J_{rel}$
	$\sigma(295K)^a$	$\sigma = f(T)$		$\sigma(295K)^a$	$\sigma = f(T)$	
15	$5.304 \cdot 10^{-11}$	$3.080 \cdot 10^{-11}$	.581	$1.347 \cdot 10^{-13}$	$8.473 \cdot 10^{-14}$	.629
20	$6.845 \cdot 10^{-10}$	$4.194 \cdot 10^{-10}$	.613	$1.258 \cdot 10^{-11}$	$7.515 \cdot 10^{-12}$	.597
25	$4.472 \cdot 10^{-9}$	$3.004 \cdot 10^{-9}$	.672	$3.133 \cdot 10^{-10}$	$2.023 \cdot 10^{-9}$	.646
30	$1.815 \cdot 10^{-8}$	$1.319 \cdot 10^{-8}$	.727	$3.388 \cdot 10^{-9}$	$2.357 \cdot 10^{-8}$	.696
35	$5.010 \cdot 10^{-8}$	$3.966 \cdot 10^{-8}$	.792	$1.836 \cdot 10^{-8}$	$1.399 \cdot 10^{-8}$	.762
40	$9.959 \cdot 10^{-8}$	$8.533 \cdot 10^{-8}$	.857	$5.601 \cdot 10^{-8}$	$4.664 \cdot 10^{-8}$	.833
45	$1.504 \cdot 10^{-7}$	$1.372 \cdot 10^{-7}$	.913	$1.036 \cdot 10^{-7}$	$9.287 \cdot 10^{-8}$	.896
50	$1.980 \cdot 10^{-7}$	$1.856 \cdot 10^{-7}$	.937	$1.492 \cdot 10^{-7}$	$1.380 \cdot 10^{-7}$	.925

$C_2F_5Cl$

Z(km)	sec $\chi = 1$			sec $\chi = 2$		
	$J(s^{-1})$	$J(s^{-1})$	$J_{rel}$	$J(s^{-1})$	$J(s^{-1})$	$J_{rel}$
	$\sigma(295K)^a$	$\sigma = f(T)$		$\sigma(295K)^a$	$\sigma = f(T)$	
15	$2.720 \cdot 10^{-13}$			$7.404 \cdot 10^{-17}$		
20	$1.337 \cdot 10^{-11}$			$1.109 \cdot 10^{-13}$		
25	$1.376 \cdot 10^{-10}$			$7.398 \cdot 10^{-12}$		
30	$6.603 \cdot 10^{-10}$			$1.097 \cdot 10^{-10}$		
35	$1.964 \cdot 10^{-9}$			$6.675 \cdot 10^{-10}$		
40	$4.081 \cdot 10^{-9}$			$2.153 \cdot 10^{-9}$		
45	$6.414 \cdot 10^{-9}$			$4.118 \cdot 10^{-9}$		
50	$8.766 \cdot 10^{-9}$			$6.317 \cdot 10^{-9}$		

<sup>a</sup> Temperature independant cross-section.

$J_{rel}$  : relative values  $J(T)/J(295K)$